LETTER

doi:10.1038/nature15758

Migratory neuronal progenitors arise from the neural plate borders in tunicates

Alberto Stolfi[1], Kerrianne Ryan[2], Ian A. Meinertzhagen[2] & Lionel Christiaen[1]

The neural crest is an evolutionary novelty that fostered the emergence of vertebrate anatomical innovations such as the cranium and jaws[1]. During embryonic development, multipotent neural crest cells are specified at the lateral borders of the neural plate before delaminating, migrating and differentiating into various cell types. In invertebrate chordates (cephalochordates and tunicates), neural plate border cells express conserved factors such as *Msx, Snail* and *Pax3/7* and generate melanin-containing pigment cells[2–4], a derivative of the neural crest in vertebrates. However, invertebrate neural plate border cells have not been shown to generate homologues of other neural crest derivatives. Thus, proposed models of neural crest evolution postulate vertebrate-specific elaborations on an ancestral neural plate border program, through acquisition of migratory capabilities and the potential to generate several cell types[5–7]. Here we show that a particular neuronal cell type in the tadpole larva of the tunicate *Ciona intestinalis*, the bipolar tail neuron, shares a set of features with neural-crest-derived spinal ganglia neurons in vertebrates. Bipolar tail neuron precursors derive from caudal neural plate border cells, delaminate and migrate along the paraxial mesoderm on either side of the neural tube, eventually differentiating into afferent neurons that form synaptic contacts with both epidermal sensory cells and motor neurons. We propose that the neural plate borders of the chordate ancestor already produced migratory peripheral neurons and pigment cells, and that the neural crest evolved through the acquisition of a multipotent progenitor regulatory state upstream of multiple, pre-existing neural plate border cell differentiation programs.

Progenitor cells that fulfil all the criteria defining the neural crest have not been observed outside vertebrates. These criteria include an embryonic origin at the lateral borders of the neural plate, epithelium-to-mesenchyme transition (EMT), migratory behaviour and the potential to differentiate into diverse cell types such as neurons, bone, cartilage and pigment cells.

In cephalochordates (amphioxus) and the tunicates *Halocynthia* and *Ciona*, a subset of neural plate border cells deploy a conserved melanocyte-specific gene network but do not migrate away from the neural tube[2–4]. Instead, they contribute locally to pigmented photoreceptor organs. In *Ciona*, the pigment cell precursors undergo an epithelial-to-mesenchymal transition and remain inside the neural tube lumen, but can be induced to exit the neural tube through targeted mis-expression of the mesenchyme-specific transcription factor Twist-related[4]. Migratory pigment cell precursors have also been reported in larvae of the tunicate *Ecteinascidia turbinata*[8].

In contrast, invertebrate homologues of neural-crest-derived neurons have so far proved elusive. In tunicates, various neurons arise from the neural plate borders, but these remain in the dorsal neural tube or in the epidermis[9,10], instead of delaminating and migrating as would be expected for homologues of vertebrate neural-crest-derived neurons. Migratory sensory neurons have been described in cephalochordate embryos, but these arise from ventral epidermis, not the neural plate borders, and reinsert into the epidermis after migrating[11].

The recently identified bipolar tail neurons (BTNs)[12] of *Ciona* larvae form axon fascicles that extend along the length of the tail on either side of the neural tube (Fig. 1a). These neurons express the proneural basic helix–loop–helix transcription factor Neurogenin (Neurog, Fig. 1b) and the LIM-homeodomain factor Islet (Fig. 1a). Vertebrate Neurogenin and Islet orthologues are involved in specifying various neuronal subtypes including neural-crest-derived dorsal root ganglia neurons (DRGNs), which also have a bipolar or pseudo-unipolar morphology and transmit peripheral mechanosensory inputs to the central nervous system[13]. *Ciona* BTNs also express *Asic*, the orthologue of acid-sensing ion channels (ASICs)[14] that modulate touch sensitivity in vertebrate DRGNs. These parallels prompted us to investigate the embryological origins of the BTNs.

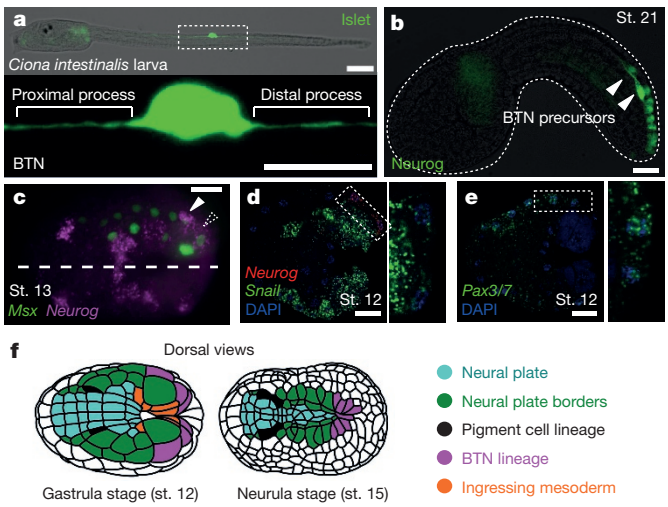

Figure 1 | Bipolar tail neurons come from the borders of the neural plate. **a**, Larva with a BTN labelled by *Islet BTN>unc-76::eGFP* (green). Bottom, enlarged view of BTN above. Scale bars, 75 µm (top); 25 µm (bottom). **b**, Migrating BTN precursors (arrowheads) labelled by the b-line-specific *Neurog b-line>unc-76::Venus* reporter construct (green). Scale bar, 25 µm. **c**, *In situ* hybridization for *Neurog* (magenta) in an embryo electroporated with *Msx>nls::lacZ* plasmid (immunolabelling of β-galactosidase in green). White arrowhead, *Msx*$^{+}$/*Neurog*$^{+}$ BTN progenitor. Dashed arrowhead, transient *Neurog* expression in BTN progenitor's sister cell (epidermal progenitor). Dashed line, midline. Scale bar, 25 µm. **d**, *In situ* hybridization for *Neurog* (red) and *Snail* (green). Scale bar, 25 µm. Inset is enlarged box showing low levels of *Snail* expression in BTN progenitor. **e**, *Pax3/7 in situ* hybridization (green). Scale bar, 25 µm. Enlarged box inset showing *Pax3/7* expression in BTN progenitor. **f**, Adapted illustration[17] of embryos showing position of pigment cell and BTN progenitors (and their descendants) in the neural plate borders. Lateral views in **a**, **b**, dorsal views in **c**–**f**. Anterior to the left throughout; st., stage.

[1]Center for Developmental Genetics, Department of Biology, New York University, New York, New York 10003, USA. [2]Department of Psychology and Neuroscience, Life Sciences Centre, Dalhousie University, Halifax, Nova Scotia B3H 4R2, Canada.

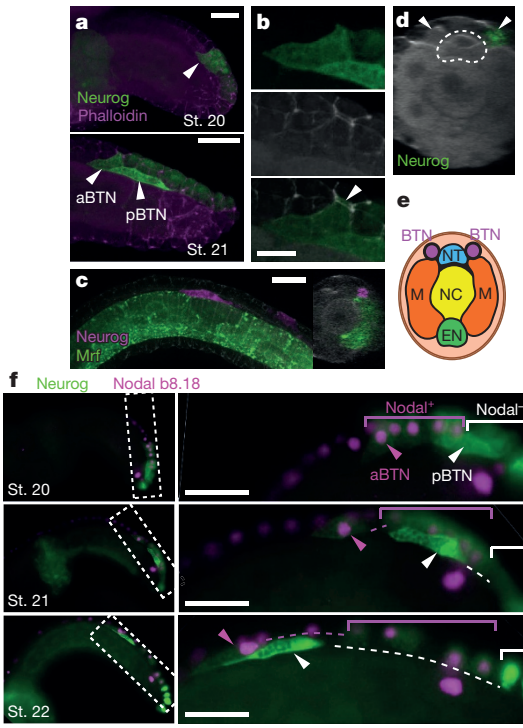

Figure 2 | Bipolar tail neuron precursors delaminate and migrate. **a**, Embryos electroporated with *Neurog b-line>unc-76::eGFP*. Top, BTN precursor (arrowhead) extending a lamellipodium. Bottom, BTN precursors (anterior (aBTN) and posterior (pBTN)) delaminating. Scale bar, 25 µm. **b**, Enlarged view of aBTN in lower panel of **a**. Top, UNC-76::eGFP; middle, phalloidin; bottom, merged; arrowhead, part of aBTN still in the epithelium. Scale bar, 10 µm. **c**, Embryo with paraxial mesoderm labelled by *Mrf>unc-76::eGFP* (green), BTN labelled by *Neurog b-line>unc-76::mCherry* (magenta) and phalloidin counterstain. Scale bar, 25 µm. Right, cross-sectioned 3D image of same embryo. Only the right side of the embryo was transfected. **d**, 3D slice of embryo showing BTNs (arrowheads) outside neural tube (dotted outline). Only the right side of the embryo was transfected. **e**, Diagram of **d** showing BTNs relative to other tail tissues: neural tube (NT), notochord (NC), myoblasts (M) and endoderm (EN). **f**, Time series of different embryos co-electroporated with *Neurog b-line>unc-76::VenusYFP* (green) and *Nodal b8.18>H2B::mCherry* (magenta). Right panels are enlarged views of the images on the left. Dashed lines indicate displacement from clonally related epidermal cells (indicated by colour-coded brackets). Scale bars, 25 µm.

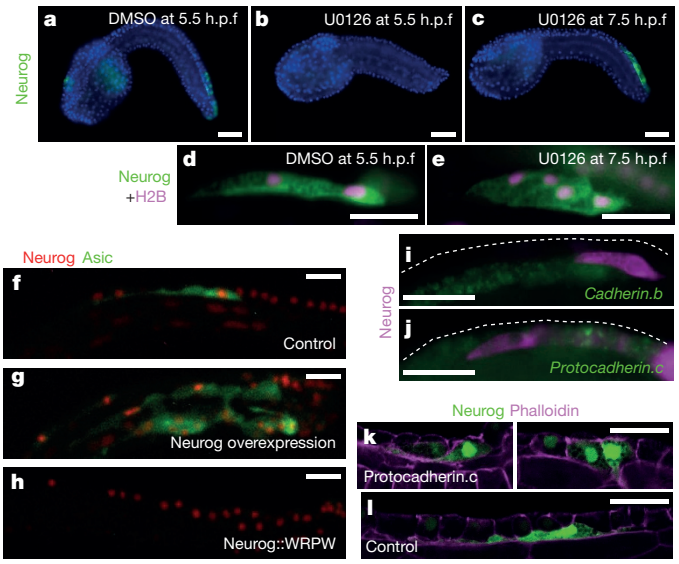

Figure 3 | Bipolar tail neuron specification and differentiation. **a**, Wild-type *Neurog b-line>unc-76::VenusYFP* expression (green) in embryos treated with DMSO vehicle, counterstained with DAPI (blue). **b**, *Neurog* expression was abolished in 43 of 50 embryos treated with 10 µM MEK inhibitor U0126 at 5.5 hours post-fertilization (h.p.f.). **c**, Supernumerary BTNs were specified in 28 of 50 embryos treated with 10 µM U0126 at 7 h.p.f. **d**, Two BTN precursors, labelled by *Neurog b-line>unc-76::VenusYFP* (green) and *Neurog b-line>H2B::mCherry* (magenta), migrating on one side of a DMSO-treated embryo. **e**, Expanded chain of four BTNs resulting from treatment with U0126 at 7 h.p.f. **f**, BTN expressing *Asic>unc-76::eGFP* reporter in embryo electroporated with *Neurog b-line>nls::lacZ* as a control. **g**, Overexpression of Neurog induces specification of ectopic *Asic*$^{+}$ BTNs in 53 of 100 embryos. **h**, Overexpression of a dominant repressor form of Neurog (Neurog::WRPW) abolishes BTNs in 97 of 100 embryos. **i**, **j**, *In situ* hybridization reveals expression of *Cadherin.b* (green) in the neural tube but not migrating BTN precursors (**i**) and expression of *Protocadherin.c* (green) in dorsal epidermis midline but not BTNs (**j**). Embryos in **i**, **j** electroporated with *Neurog b-line>unc-76::mCherry* (immunolabelling of mCherry in magenta). **k**, Forced overexpression of protocadherin.c in the BTN lineage using the *Neurog b-line* driver inhibits delamination and migration of BTNs in 7 of 14 embryos. **l**, Normal BTNs as seen in 9 of 12 control embryos (overexpression of β-galactosidase instead). Embryos in **k**, **l** electroporated with *Neurog b-line>unc-76::VenusYFP* and *Neurog b-line>H2B::VenusYFP* (green) and counterstained with phalloidin (magenta). All scale bars 25 µm. Embryos in **a**–**e**, **i**, **j** fixed at stage 22. Embryos in **f**–**h**, **k**, **l** at stage 23.

We detected the earliest expression of *Neurog* at neurulation, in the caudal-most neural/epidermal boundary cells, which express the conserved neural plate border specification genes *Msx*[15], *Pax3/7* (ref. 3) and *Snail*[16] (Fig. 1c–f and Extended Data Fig. 1). During neurulation, these cells drive neural tube closure and their progeny eventually form the neural tube roof plate and dorsal epidermis midline[17,18] (Fig. 1b and Extended Data Fig. 2). BTN progenitors are thus born from the caudal extensions of the lateral borders of the neural plate (Fig. 1f).

We isolated a *Neurog cis*-regulatory element that drives reporter gene expression in this caudal neural plate border region (Extended Data Fig. 3). Using this reporter, we determined that *Neurog* expression is progressively restricted and maintained in only two cells on each side of the bilaterally symmetric embryo, born during neural tube closure (Extended Data Figs 2 and 4). We have named these the anterior (aBTN) and posterior (pBTN) BTN precursors. Shortly after the completion of neural tube closure, BTN precursors delaminate and migrate anteriorly along the paraxial mesoderm on either side of the neural tube[19] (Fig. 2a–f and Supplementary Videos 1–3). This is evocative of vertebrate DRGN progenitors, which migrate through paraxial mesoderm situated lateral to the neural tube.

Double-labelling with a *Nodal* reporter revealed that BTNs arise from two adjacent but clonally distinct cell lineages (Fig. 2g and Extended Data Fig. 2). The pBTN arises from the tail tip (b8.21 lineage)[10] and migrates to meet the b8.18-derived aBTN as it delaminates (Fig. 2a, f). Together, they continue their migration as a chain of two cells.

Neurog expression distinguishes the BTNs from the caudal epidermal sensory neurons (CESNs), which remain at the dorsal midline and are specified instead by an atonal homologue (Atoh)-dependent regulatory program[10,20]. We found that the onset of *Neurog* expression requires MAPK/ERK signalling (Fig. 3a, b). However, later inhibition of MAPK/ERK resulted in the upregulation of *Neurog* in non-neural cells of the lineage, converting these into supernumerary BTNs (Fig. 3c–e and Extended Data Fig. 4). In contrast, perturbing Delta/Notch signalling did not alter BTN specification or differentiation (Extended Data Fig. 5). Overexpression of Neurog also induced ectopic migratory *Asic*$^{+}$ BTN precursors (Fig. 3f, g), while BTNs were abolished through expression of a dominant repressor form of Neurog (Neurog::WRPW, Fig. 3h). In all cases, induced supernumerary BTN precursors migrated as an expanded chain of cells (Fig. 3e, g). These data indicate that sustained *Neurog* expression in caudal neural plate border cells is controlled by MAPK/ERK signalling and is necessary and sufficient for BTN specification, migration and differentiation.

In vertebrates, neural crest EMT is effected in part through differential cell adhesion, mediated by various mechanisms regulating cadherin

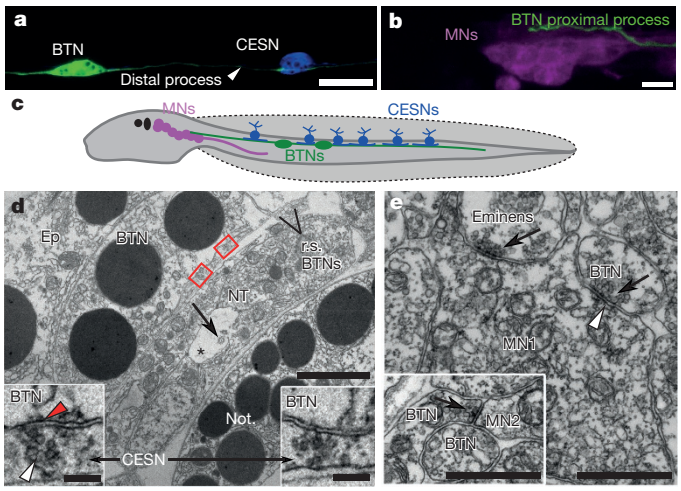

Figure 4 | Synaptic connections of bipolar tail neurons. a, BTN labelled by *Gad>unc-76::eGFP* (green) contacting a CESN labelled by *Slc17a6/7/8(Vglut)>unc-76::mCherry* (blue). **b**, Proximal process of BTN labelled by *Islet BTN>unc-76::mCherry* (green) contacting motor neurons (MNs) labelled by *Fgf8/17/18> unc-76::eGFP* (magenta). **c**, Diagram of *Ciona* larva showing synaptic connections between CESNs in tail epidermis, BTNs and MNs. **d**, Two synaptic inputs (red boxes, insets) from the sheet-like profile of a CESN to a left-side BTN; transmission electron micrograph from wide-area montage. The profile of a second BTN axon lies out of view. Axon profiles from two right-side BTN axons (r.s. BTNs) are visible. BTNs overlie the neural tube (NT) with neural canal (marked with an asterisk) and cross-sectioned cilia (arrow). An epidermal cell (Ep) overlies the BTN. Each synapse enlarged in inset has ~52 nm diameter presynaptic vesicles (white arrowhead), and the left synapse has a postsynaptic density (red arrowhead). Scale bars, 1 µm (inset scale bars, 0.5 µm). Not., notochord. **e**, Synaptic input (arrow) from a BTN to the axon of a member of the most anterior pair (A11.118) of motor neurons (MN1), identified by a cumulus of ~60-nm presynaptic vesicles and a shallow postsynaptic density (arrowhead). A second input nearby originates from the axon of an eminens neuron[12] (arrow). Inset, synaptic input from BTN to the axon of a second pair of motor neurons (MN2). Scale bars, 1 µm.

function[21]. We found that expression of *Cadherin.b*, the predominant cadherin gene expressed in the neural tube of *Ciona* embryos, is absent in BTN precursors (Fig. 3i). Moreover, BTN precursors do not express *Protocadherin.c*, a cadherin superfamily gene expressed in CESNs and epidermis midline (Fig. 3j). Overexpression of protocadherin.c protein inhibited delamination and migration of BTNs (Fig. 3k, l), suggesting that *Ciona* BTNs and vertebrate neural crest share regulatory strategies for EMT via differential cell–cell adhesion.

We observed that each BTN precursor initially migrates anteriorly with a prominent leading edge that becomes the cell's anterior neurite (or 'proximal process'), while its Golgi apparatus is located posterior to the cell nucleus. At around 12 h post-fertilization, each BTN precursor undergoes a 180° polarity inversion, with the Golgi repositioning itself anterior to the nucleus immediately before the cell begins to elaborate the posterior segment of its neurite (the 'distal process'), resulting in a bipolar morphology (Extended Data Fig. 6, Supplementary Video 4 and Supplementary Table 1). These observations suggest that a precisely timed re-orientation of cell polarity underlies the characteristic bipolar morphology of the BTNs.

At hatching, BTN cell bodies are situated in the middle of the tail along the anterior–posterior axis, with their distal processes extending towards the tail tip and proximal processes projecting towards the motor ganglion and brain (Fig. 4a–c)[12]. Electron microscopy confirmed that the BTN somata lie outside the neural tube and are invariably overlain by epidermal cells (Fig. 4d). BTNs lack junctions with epidermal cells and also lack cilia, thus failing to penetrate the tunic to contact the exterior. These characteristics suggest that while distal BTN neurites may be sensory, their cell bodies lack epidermal sensory receptors found in CESNs[22]. Along the tail, the BTNs contact overlying CESNs, the short processes of which do not reach the motor ganglion[12] (Fig. 4a–c). At these contacts, synapses form from the CESN to the BTNs (Fig. 4d). Unlike the CESNs, the proximal processes of the BTNs form synaptic contacts with the motor neurons that innervate and control the tail muscles (Fig. 4b, c, e). Each BTN establishes many such contacts upon the two most anterior pairs of motor neurons, MN1 and MN2, on both the left and right sides (Fig. 4e and Extended Data Table 1). These synaptic connections are similar to those of mammalian slowly adapting type I DRGNs that, in addition to being mechanosensitive themselves, relay distinct inputs from mechanosensory Merkel cells of the epidermis[23]. Both tunicate CESNs and vertebrate Merkel cells arise from non-migratory epidermal cells, require Atoh factors for their specification and are glutamatergic in their neurotransmitter phenotype[10,20,24,25]. These data suggest that tunicate BTNs may thus be equivalent to vertebrate DRGNs within a homologous ascending sensory pathway (Fig. 4c).

In anamniote vertebrates, evidence for a common progenitor of intramedullary Rohon–Beard neurons (RBNs) and neural crest, in addition to other similarities between RBNs and DRGNs, indicates a deep homology between these cell types[26]. Fritzsch and Northcutt proposed that a key step in the evolution of neural crest was the elaboration of extramedullary sensory neurons from intramedullary RBN-like neurons[27]. Following the Fritzsch–Northcutt model, the BTNs may be derived from an 'intermediate' extramedullary neuron that evolved in the last common ancestor of Olfactores (vertebrates and tunicates) before the appearance of bona fide neural crest in the vertebrates. The migration of BTN precursors along the paraxial mesoderm, similar to later phases of DRGN migration, suggests that some of the diverse EMT and migratory behaviours displayed by vertebrate neural crest cells may pre-date the emergence of vertebrates.

Although the embryological origin (neural plate borders) and molecular signature (*Neurog*$^{+}$/*Islet*$^{+}$) of the BTNs of *Ciona* also support homology with RBNs, the two do in fact differ in several key aspects. First, BTNs are extramedullary neurons derived from progenitor cells that migrate along paraxial mesoderm lateral to the neural tube. Second, expression of ASICs is shared between BTNs and DRGNs, but appears absent from RBNs[28]. Finally, RBNs are multipolar with extensively branching peripheral neurites that innervate the overlying epidermis[29], while we have not observed any peripheral neurites projecting from the bipolar/pseudounipolar BTNs.

We have revealed the developmental history of migratory neuronal progenitors that arise from the neural plate borders of tunicate embryos. Based on their embryological origin, gene expression, cell behaviour, morphology and synaptic connections, we propose that the BTNs are homologous to neural-crest-derived DRGNs. This would imply that the neural plate borders of the olfactorean ancestor gave rise to at least two types of neural crest derivatives: pigment cells and peripheral neurons (Extended Data Fig. 7).

In the invariantly developing *Ciona* embryo, the pigment cell and BTN lineages become separated early in development, but converge at a neural plate border cell identity before parting again towards distinct differentiated fates. This separation between the two lineages may represent the ancestral condition of the neural plate borders before the evolution of the neural crest in vertebrates. This would support models that propose an evolutionary origin for vertebrate neural crest through a heterochronic shift or 'intercalation' of a multipotent progenitor state downstream of neural plate border specification but upstream of cell differentiation, based on shared regulatory programs between neural crest and pluripotent cells of the early embryo[1,30].

Online Content Methods, along with any additional Extended Data display items and Source Data, are available in the online version of the paper; references unique to these sections appear only in the online paper.

Received 25 March; accepted 30 September 2015.
Published online 28 October; corrected online 18 November 2015 (see full-text HTML version for details).

1. Bronner, M. E. & LeDouarin, N. M. Evolution and development of the neural crest: an overview. *Dev. Biol.* **366,** 2–9 (2012).
2. Yu, J.-K., Meulemans, D., McKeown, S. J. & Bronner-Fraser, M. Insights from the amphioxus genome on the origin of vertebrate neural crest. *Genome Res.* **18,** 1127–1132 (2008).
3. Wada, H., Holland, P. W. H., Sato, S., Yamamoto, H. & Satoh, N. Neural tube is partially dorsalized by overexpression of *HrPax-37*: the ascidian homologue of *Pax-3* and *Pax-7*. *Dev. Biol.* **187,** 240–252 (1997).
4. Abitua, P. B., Wagner, E., Navarrete, I. A. & Levine, M. Identification of a rudimentary neural crest in a non-vertebrate chordate. *Nature* **492,** 104–107 (2012).
5. Wada, H. Origin and evolution of the neural crest: a hypothetical reconstruction of its evolutionary history. *Dev. Growth Differ.* **43,** 509–520 (2001).
6. Baker, C. V. H. & Bronner-Fraser, M. The origins of the neural crest. Part II: an evolutionary perspective. *Mech. Dev.* **69,** 13–29 (1997).
7. Shimeld, S. M. & Holland, P. W. H. Vertebrate innovations. *Proc. Natl Acad. Sci. USA* **97,** 4449–4452 (2000).
8. Jeffery, W. R., Strickler, A. G. & Yamamoto, Y. Migratory neural crest-like cells form body pigmentation in a urochordate embryo. *Nature* **431,** 696–699 (2004).
9. Mazet, F. *et al.* Molecular evidence from *Ciona intestinalis* for the evolutionary origin of vertebrate sensory placodes. *Dev. Biol.* **282,** 494–508 (2005).
10. Pasini, A. *et al.* Formation of the ascidian epidermal sensory neurons: insights into the origin of the chordate peripheral nervous system. *PLoS Biol.* **4,** e225 (2006).
11. Kaltenbach, S. L., Yu, J.-K. & Holland, N. D. The origin and migration of the earliest-developing sensory neurons in the peripheral nervous system of amphioxus. *Evol. Dev.* **11,** 142–151 (2009).
12. Imai, J. H. & Meinertzhagen, I. A. Neurons of the ascidian larval nervous system in *Ciona intestinalis*: II. Peripheral nervous system. *J. Comp. Neurol.* **501,** 335–352 (2007).
13. Ma, Q., Fode, C., Guillemot, F. & Anderson, D. J. NEUROGENIN1 and NEUROGENIN2 control two distinct waves of neurogenesis in developing dorsal root ganglia. *Genes Dev.* **13,** 1717–1728 (1999).
14. Coric, T., Passamaneck, Y. J., Zhang, P., Di Gregorio, A. & Canessa, C. M. Simple chordates exhibit a proton-independent function of acid-sensing ion channels. *FASEB J.* **22,** 1914–1923 (2008).
15. Aniello, F. *et al.* Identification and developmental expression of *Ci-msxb:* a novel homologue of *Drosophila msh* gene in *Ciona intestinalis*. *Mech. Dev.* **88,** 123–126 (1999).
16. Wada, S. & Saiga, H. Cloning and embryonic expression of *Hrsna*, a *snail* family gene of the ascidian *Halocynthia roretzi*: implication in the origins of mechanisms for mesoderm specification and body axis formation in chordates. *Dev. Growth Differ.* **41,** 9–18 (1999).
17. Hashimoto, H., Robin, F. B., Sherrard, K. M. & Munro, E. M. Sequential contraction and exchange of apical junctions drives zippering and neural tube closure in a simple chordate. *Dev. Cell* **32,** 241–255 (2015).
18. Nicol, D. & Meinertzhagen, I. Development of the central nervous system of the larva of the ascidian, *Ciona intestinalis* L: II. Neural plate morphogenesis and cell lineages during neurulation. *Dev. Biol.* **130,** 737–766 (1988).
19. Nakamura, M. J., Terai, J., Okubo, R., Hotta, K. & Oka, K. Three-dimensional anatomy of the *Ciona intestinalis* tailbud embryo at single-cell resolution. *Dev. Biol.* **372,** 274–284 (2012).
20. Tang, W. J., Chen, J. S. & Zeller, R. W. Transcriptional regulation of the peripheral nervous system in *Ciona intestinalis*. *Dev. Biol.* **378,** 183–193 (2013).
21. Theveneau, E. & Mayor, R. Neural crest delamination and migration: from epithelium-to-mesenchyme transition to collective cell migration. *Dev. Biol.* **366,** 34–54 (2012).
22. Torrence, S. & Cloney, R. Nervous system of ascidian larvae: caudal primary sensory neurons. *Zoomorphology* **99,** 103–115 (1982).
23. Maksimovic, S. *et al.* Epidermal Merkel cells are mechanosensory cells that tune mammalian touch receptors. *Nature* **509,** 617–621 (2014).
24. Morrison, K. M., Miesegaes, G. R., Lumpkin, E. A. & Maricich, S. M. Mammalian Merkel cells are descended from the epidermal lineage. *Dev. Biol.* **336,** 76–83 (2009).
25. Horie, T., Kusakabe, T. & Tsuda, M. Glutamatergic networks in the *Ciona intestinalis* larva. *J. Comp. Neurol.* **508,** 249–263 (2008).
26. Artinger, K. B., Chitnis, A. B., Mercola, M. & Driever, W. Zebrafish narrowminded suggests a genetic link between formation of neural crest and primary sensory neurons. *Development* **126,** 3969–3979 (1999).
27. Fritzsch, B. & Northcutt, R. G. Cranial and spinal nerve organization in amphioxus and lampreys: evidence for an ancestral craniate pattern. *Acta Anat. (Basel)* **148,** 96–109 (1993).
28. Paukert, M. *et al.* A family of acid-sensing ion channels from the zebrafish: widespread expression in the central nervous system suggests a conserved role in neuronal communication. *J. Biol. Chem.* **279,** 18783–18791 (2004).
29. O'Brien, G. S. *et al.* Coordinate development of skin cells and cutaneous sensory axons in zebrafish. *J. Comp. Neurol.* **520,** 816–831 (2012).
30. Buitrago-Delgado, E., Nordin, K., Rao, A., Geary, L. & LaBonne, C. Shared regulatory programs suggest retention of blastula-stage potential in neural crest cells. *Science* **348,** 1332–1335 (2015).

Supplementary Information is available in the online version of the paper.

Acknowledgements The authors would like to thank F. Razy-Krajka for assistance with Kaede photoconversion and comments on the manuscript, T. Tolkin for constructing the *Mrf* reporter plasmid, Z. Lu for ultramicrotomy, and C. Desplan, A. Di Gregorio and all members of the Christiaen and Meinertzhagen labs for feedback and suggestions. We thank H. Hashimoto, F. Robin and N. Takatori for embryo illustration template files. This work was funded by a National Science Foundation Postdoctoral Fellowship in Biology (under grant NSF-1161835) to A.S., by National Institutes of Health award GM096032 to L.C., and by grant DIS0000065 from NSERC (Ottawa) to I.A.M.

Author Contributions A.S., K.R., I.A.M. and L.C. designed the study, analysed the data, and wrote the paper. A.S. and K.R. performed the experiments.

Author Information Reprints and permissions information is available at www.nature.com/reprints. The authors declare no competing financial interests. Readers are welcome to comment on the online version of the paper. Correspondence and requests for materials should be addressed to L.C. (lc121@nyu.edu).

METHODS

Molecular cloning. Reporter constructs were designed based on information of *cis*-regulatory modules (CRMs) from previously published studies on the following genes: *Islet*[31], *Msx*[32], *Neurog*[33], *Nodal*[34], *Asic*[14], glutamate decarboxylase (*Gad*)[35], Slc17a6/7/8 (*Vglut*)[25] and *Fgf8/17/18* (ref. 36). The *Neurog b-line* CRM (Ciinte.REG.KhC6.1500090-1502346) was cloned using the following primers: *Neurog* −3,010 forward (5′-GTCTGTTTCCGCATACATGC-3′) and *Neurog* −773 reverse (5′-CTTATACGCCGAACCTCATG-3′). The *Neurog b-line* minimal CRM (Ciinte.REG.KhC6.1500090-1500501) was found to be contained within this region and cloned using *Neurog* −3,010 forward and *Neurog* −2,599 reverse (5′-GCAAAACGTTTCCCGATTCG-3′) primers. *Neurog* CRMs were cloned upstream of the basal promoter of *Neurog* (Ciinte.REG.KhC6.1502506-1503107), cloned using the primers *Neurog* −594 forward (5′-GGTCATGCTTTGTTACGTCC-3′) and *Neurog* +9 reverse (5′-ATCCAACATTTTGTAGCAAGAGC-3′), or the basal promoter of the *Zfpm* gene (also known as friend of GATA, or *Fog*)[37]. The full-length *Mrf* CRM (Ciinte.REG.KhC14.4311719-4314636) was cloned using the primers (5′-GCAAGCTCCTTTGGGGTTTGG-3′) and (5′-CGTATAAATATGTCAAACTACCGGC-3′). *Caenorhabditis elegans* UNC-76 tags were fused to fluorescent proteins to ensure even labelling of axons[38]. Probes used for *in situ* hybridization were transcribed *in vitro* from templates obtained from previously published gene collection clones[39,40] for *Neurog* (R1CiGC29n04), *Pax3/7* (R1CiGC42e20), *Ebf* (R1CiGC02i14) and *Cadherin.b* (VES104_F13) or cloned *de novo* from coding sequences for *Snail* (KH.C3.751.v1.C.SL1-1) and *Protocadherin.c* (KH.C9.32.v1.A.SL1-1). Golgi-targeting sequence was cloned from KH.C14.396.v1.B.ND1-1 cDNA (*N*-acetylgalactosaminyltransferase 7, or *Galnt7*) using the primers *Galnt7* amino acid 1 forward (5′-ATGAGATTTAAAATCGCATCAGTTTTG-3′) and *Galnt7* amino acid 157 reverse (5′-AAGTGATATCTTGTCGCTGTTCAC-3′) and fused in-frame to fluorescent proteins. *Neurog* coding sequence and *Neurog::WRPW* have been previously cloned and published[41]. *dnFGFR* has been previously published[42], as has *Su(H)-DBM*[43].

Embryo handling, *in situ* hybridization and immunolabelling. For purposes other than for electron microscopy (see below), eggs and embryos from wild-caught *Ciona intestinalis* (species type A, '*robusta*') purchased from M-REP (San Diego, California) were handled according to established protocols[44]. Double *in situ* hybridization/immunolabelling was performed as described in previous publications[45,46]. Monoclonal anti-β-galactosidase (Promega catalogue number Z3781), rabbit polyclonal anti-mCherry (BioVision, accession number ACY24904), and Alexa Fluor-conjugated secondary antibodies (Life Technologies) were all used at 1:500 working dilution. Alexa Fluor-conjugated phalloidin (Life Technologies) was used at 1:50 working dilution. MEK inhibitor U0126 (Cell Signaling Technology) was resuspended as stock solution in DMSO at 10 mM concentration, and diluted to 10 μM in artificial sea water for embryo treatments. Sample sizes equal the total number of embryos present per microscope slide, unless these exceeded arbitrarily set limits of 50 or 100 embryos. No statistical methods were used to predetermine sample size and no replicates were used. The experiments were not randomized and the investigators were not blinded to allocation during experiments and outcome assessment.

Fluorescence/confocal microscopy and photoconversion. Images were captured on a Leica inverted TCS SP8 X confocal or DM2500 epifluorescence microscope. For time-lapse image capture, embryos were imaged as they developed in sea water-filled chambers on coverslip-bottom Petri dishes (MatTek). Confocal image stacks were processed in Leica Application Suite or ImageJ. Video annotations were made using Camtasia software (TechSmith). 3D slices and projections were generated using Imaris (Bitplane) or Volocity (PerkinElmer) software. Kaede::nls[47] was photoconverted as previously described[48]. Neurite lengths and Golgi apparatus positioning were measured using ImageJ. Not all cells, neurites and/or Golgi were visible in every embryo. Golgi positioning relative to BTN nuclei was measured in degrees of angle formed between a line traced anteriorly from the nucleus and another line traced through the middle of the Golgi complex. Thus, when the Golgi complex is perfectly aligned anterior to the nucleus, the angle is 0°, whereas if the Golgi complex is perfectly posterior to the nucleus, the angle is 180°. Rose plots (angle histograms) were generated in Matlab (http://www.mathworks.com/help/matlab/ref/rose.html).

Electron microscopy. Adult animals, *Ciona intestinalis* (L.), were collected by P. Darnell from Mahone Bay, Nova Scotia. Two-hour larvae reared at 18 °C in the dark were fixed at 4 °C for 1 h in 1% OsO_4 in 1.25% $NaHCO_3$ adjusted to pH 7.2 with HCl, followed by 2% glutaraldehyde in 0.1 M phosphate buffer. After fixation they were embedded in Epon, and a single larva cross sectioned at 60 nm in the motor ganglion and later at 100 nm down the length of the tail, and the sections post-stained for 5–6 min in freshly prepared aqueous uranyl acetate followed by 2–3 min in lead citrate. Sections were viewed using an FEI Tecnai 12 electron microscope operated at 80 kV and images captured using either a Kodak Megaview II camera using software (AnalySIS: SIS GmbH), or a Gatan 832 Orius SC1000 CCD camera using Gatan DigitalMicrograph software to compile multi-panel montages from each section. Comprehensive electron micrograph series identified the cell bodies and axons of BTNs, motor neurons and CESNs from their positions and shapes, and these in turn enabled identification of their connections (K.R. and I.A.M., manuscript in preparation).

31. Stolfi, A. *et al.* Early chordate origins of the vertebrate second heart field. *Science* **329,** 565–568 (2010).
32. Russo, M. T. *et al.* Regulatory elements controlling *Ci-msxb* tissue-specific expression during *Ciona intestinalis* embryonic development. *Dev. Biol.* **267,** 517–528 (2004).
33. Stolfi, A. & Christiaen, L. Genetic and genomic toolbox of the chordate *Ciona intestinalis*. *Genetics* **192,** 55–66 (2012).
34. Khoueiry, P. *et al.* A *cis*-regulatory signature in ascidians and flies, independent of transcription factor binding sites. *Curr. Biol.* **20,** 792–802 (2010).
35. Takamura, K., Minamida, N. & Okabe, S. Neural map of the larval central nervous system in the ascidian *Ciona intestinalis*. *Zoolog. Sci.* **27,** 191–203 (2010).
36. Imai, K. S., Stolfi, A., Levine, M. & Satou, Y. Gene regulatory networks underlying the compartmentalization of the *Ciona* central nervous system. *Development* **136,** 285–293 (2009).
37. Rothbächer, U., Bertrand, V., Lamy, C. & Lemaire, P. A combinatorial code of maternal GATA, Ets and β-catenin-TCF transcription factors specifies and patterns the early ascidian ectoderm. *Development* **134,** 4023–4032 (2007).
38. Dynes, J. L. & Ngai, J. Pathfinding of olfactory neuron axons to stereotyped glomerular targets revealed by dynamic imaging in living zebrafish embryos. *Neuron* **20,** 1081–1091 (1998).
39. Satou, Y. *et al.* A cDNA resource from the basal chordate *Ciona intestinalis*. *Genesis* **33,** 153–154 (2002).
40. Roure, A. *et al.* A multicassette Gateway vector set for high throughput and comparative analyses in *Ciona* and vertebrate embryos. *PLoS ONE* **2,** e916 (2007).
41. Stolfi, A., Wagner, E., Taliaferro, J. M., Chou, S. & Levine, M. Neural tube patterning by Ephrin, FGF and Notch signaling relays. *Development* **138,** 5429–5439 (2011).
42. Davidson, B., Shi, W., Beh, J., Christiaen, L. & Levine, M. FGF signaling delineates the cardiac progenitor field in the simple chordate, *Ciona intestinalis*. *Genes Dev.* **20,** 2728–2738 (2006).
43. Hudson, C. & Yasuo, H. A signalling relay involving Nodal and Delta ligands acts during secondary notochord induction in *Ciona* embryos. *Development* **133,** 2855–2864 (2006).
44. Christiaen, L., Wagner, E., Shi, W. & Levine, M. The sea squirt *Ciona intestinalis*. *Cold Spring Harb. Protoc.* pdb.emo138 (2009).
45. Beh, J., Shi, W., Levine, M., Davidson, B. & Christiaen, L. *FoxF* is essential for FGF-induced migration of heart progenitor cells in the ascidian *Ciona intestinalis*. *Development* **134,** 3297–3305 (2007).
46. Ikuta, T. & Saiga, H. Dynamic change in the expression of developmental genes in the ascidian central nervous system: revisit to the tripartite model and the origin of the midbrain–hindbrain boundary region. *Dev. Biol.* **312,** 631–643 (2007).
47. Ando, R., Hama, H., Yamamoto-Hino, M., Mizuno, H. & Miyawaki, A. An optical marker based on the UV-induced green-to-red photoconversion of a fluorescent protein. *Proc. Natl Acad. Sci. USA* **99,** 12651–12656 (2002).
48. Razy-Krajka, F. *et al.* Collier/OLF/EBF-dependent transcriptional dynamics control pharyngeal muscle specification from primed cardiopharyngeal progenitors. *Dev. Cell* **29,** 263–276 (2014).
49. Nishida, H. Cell division pattern during gastrulation of the ascidian, *Halocynthia roretzi*. *Dev. Growth Differ.* **28,** 191–201 (1986).
50. Bone, Q. The central nervous system in amphioxus. *J. Comp. Neurol.* **115,** 27–64 (1960).

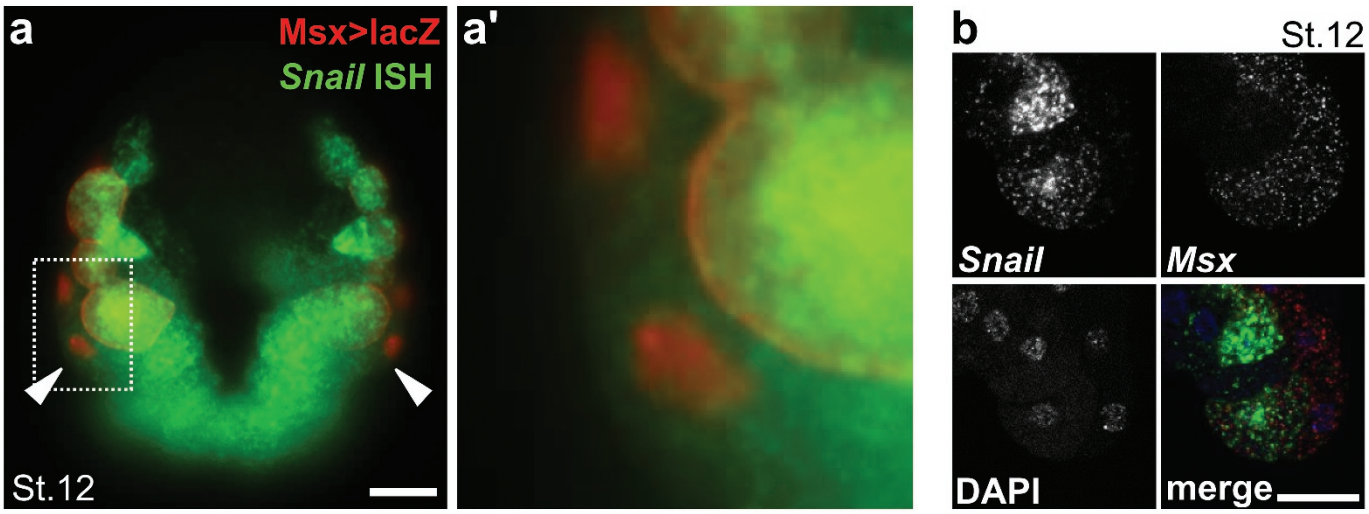

Extended Data Figure 1 | *In situ* hybridization of neural plate border markers *Snail* and *Msx*. **a**, Immunolabelling for β-galactosidase (red) and *in situ* hybridization for *Snail* mRNA (green) in stage 12 embryo electroporated with *Msx>lacZ,* revealing *Snail* expression in the BTN progenitors (b9.36 cells, arrowheads). Dashed area enlarged in **a′**. **b**, Double *in situ* hybridization for *Snail* (green on merged image) and *Msx* (red on merged image) in stage 12 embryos counterstained with DAPI (blue on merged image), showing co-expression in neural plate border cells, including BTN progenitors. Scale bars, 25 μm.

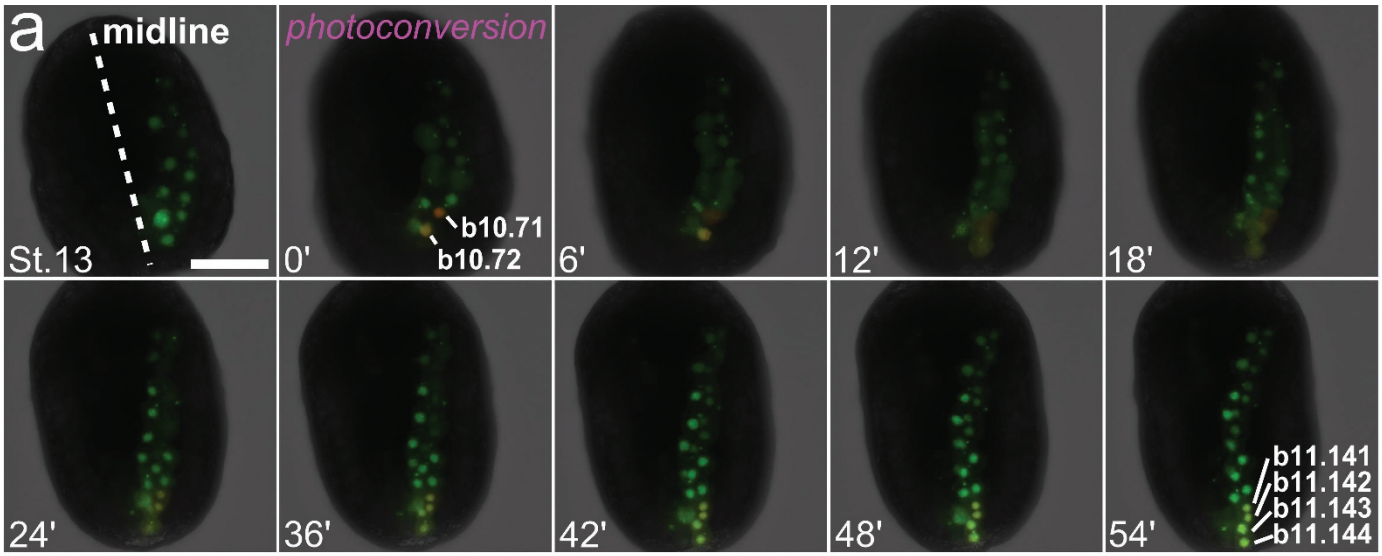

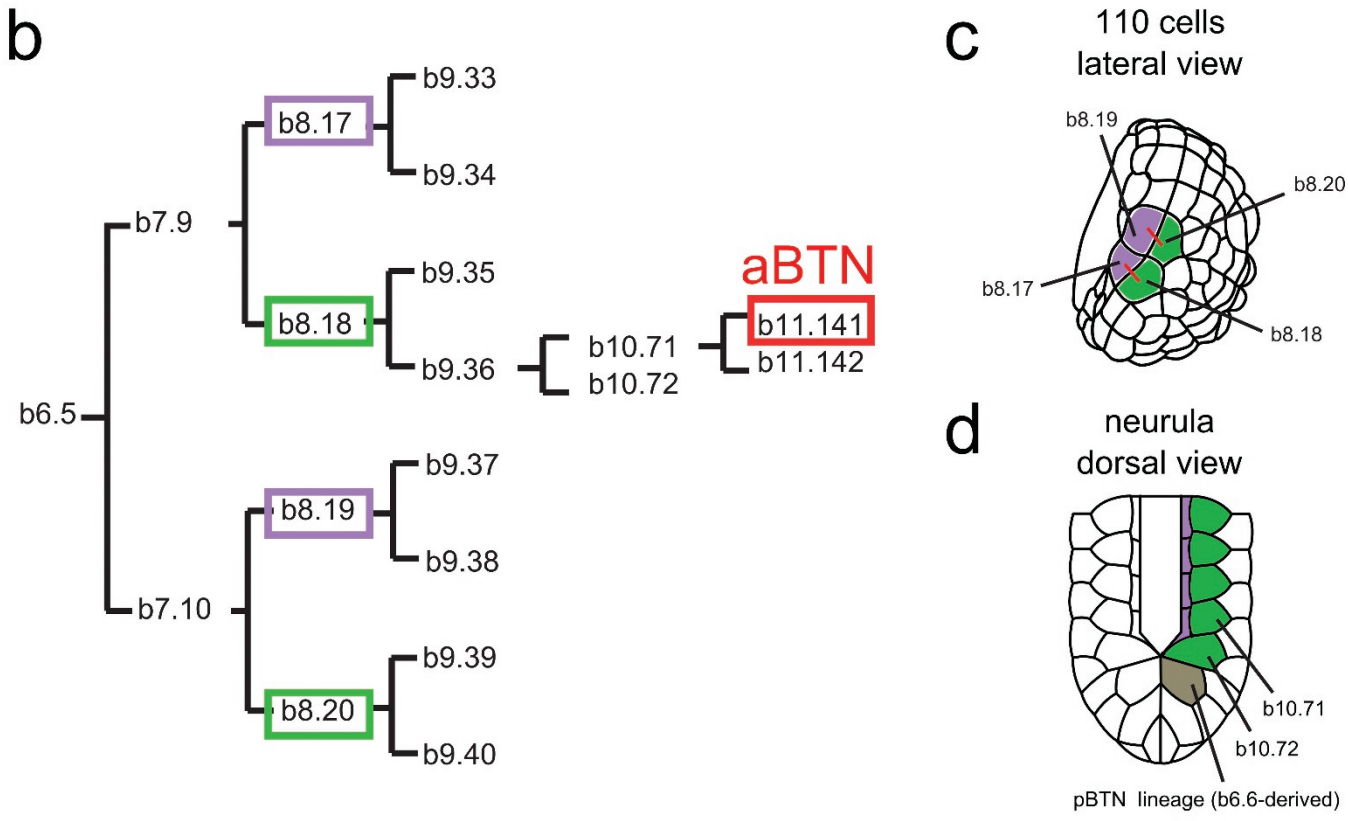

32 cells 4 hpf | 64 cells 4 hpf | 110 cells 4 hpf | gastrula 5 hpf | neurula 6 hpf | tailbud 7 hpf

Extended Data Figure 2 | Lineage tracing of b9.36 descendants. **a**, Photoconversion of Kaede::nls driven by the *Msx* driver was used to follow the cell divisions of the BTN progenitors from the late gastrula stage to the early tailbud stage. Both b10.71 and b10.72 divide once. b11.141 will give rise to a definitive anterior BTN (see Extended Data Fig. 4). Numbers in each panel represent time in minutes elapsed from the initial photoconversion event. Scale bar, 50 µm. **b**, Lineage tree showing specification of aBTNs in relation to other cells of the posterior neural plate borders. For simplicity, only one side of the embryo is depicted. **c**, Lateral view of a 110-cell-stage embryo showing the positions of blastomeres in **b**. Red lines connect sibling cells. **d**, Dorsal view of a neurula-stage embryo showing zippering of posterior neural-plate-border-derived capstone cells[18] as neural tube closure is initiated. Panels **b** and **d** are courtesy of H. Hashimoto and F. Robin (University of Chicago) and N. Takatori (Tokyo Metropolitan University), and partially modelled after ref. 17. Panel **c** modelled after ref. 49.

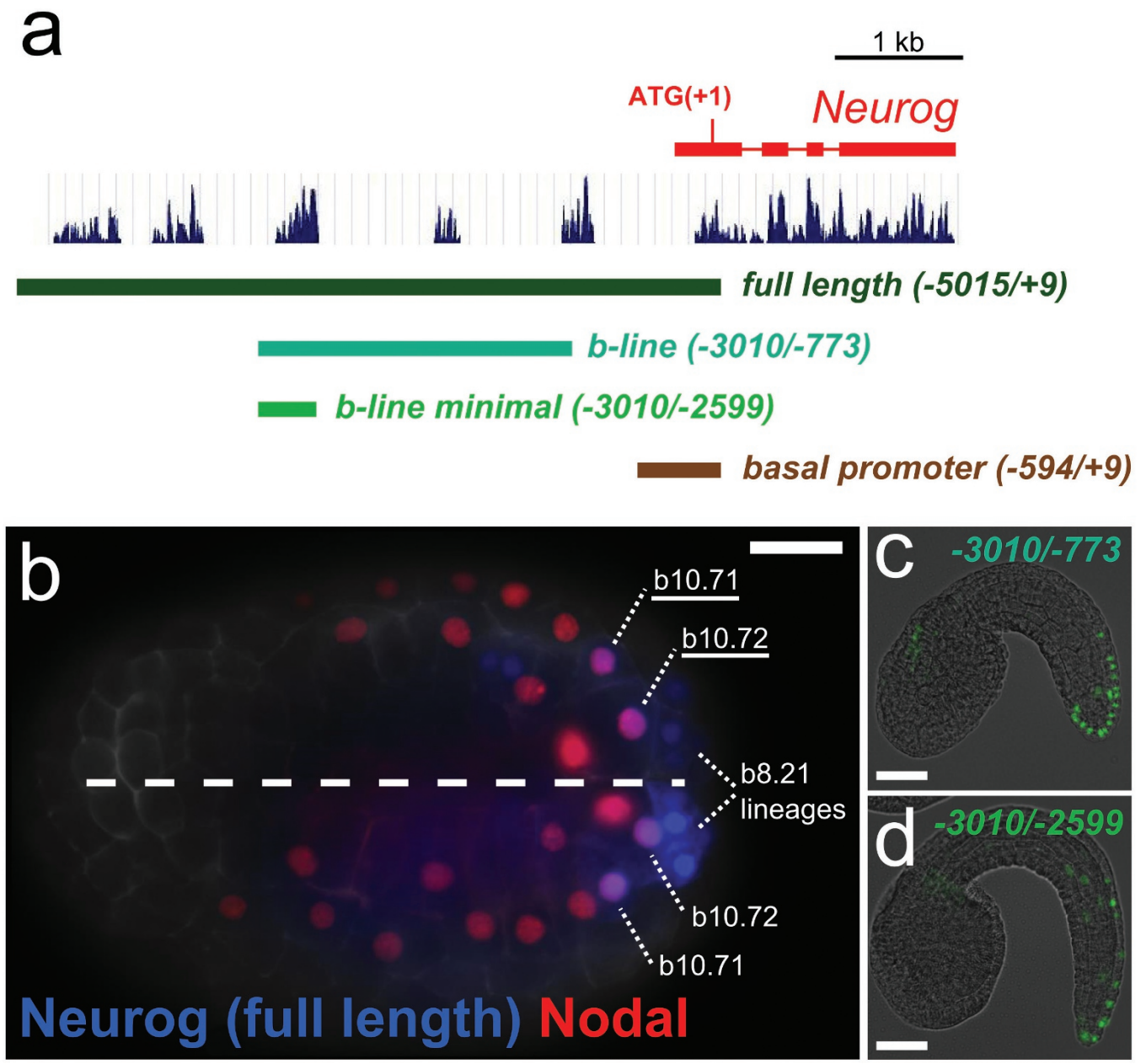

Extended Data Figure 3 | *Neurog cis*-regulatory sequences. a, Schematic diagram representing *Neurog* locus and 5′ *cis*-regulatory sequences including *b-line* and *b-line minimal cis*-regulatory modules. Peaks represent nucleotide sequence conservation with *Ciona savignyi* genome. **b**, Late gastrula embryo (stage 13) electroporated with full-length *Neurog* (blue) and *Nodal b-line* (red) reporter constructs. Reporter co-expression is seen in b9.36 descendants on either side of the neural plate. *Neurog* expression also marks tail-tip lineages of uncertain provenance, previously reported to be descended from b8.21 (ref. 10). Scale bar, 25 µm. **c**, *Neurog b-line* reporter. **d**, *Neurog b-line minimal* reporter. Scale bars in **c**, **d**, 50 µm.

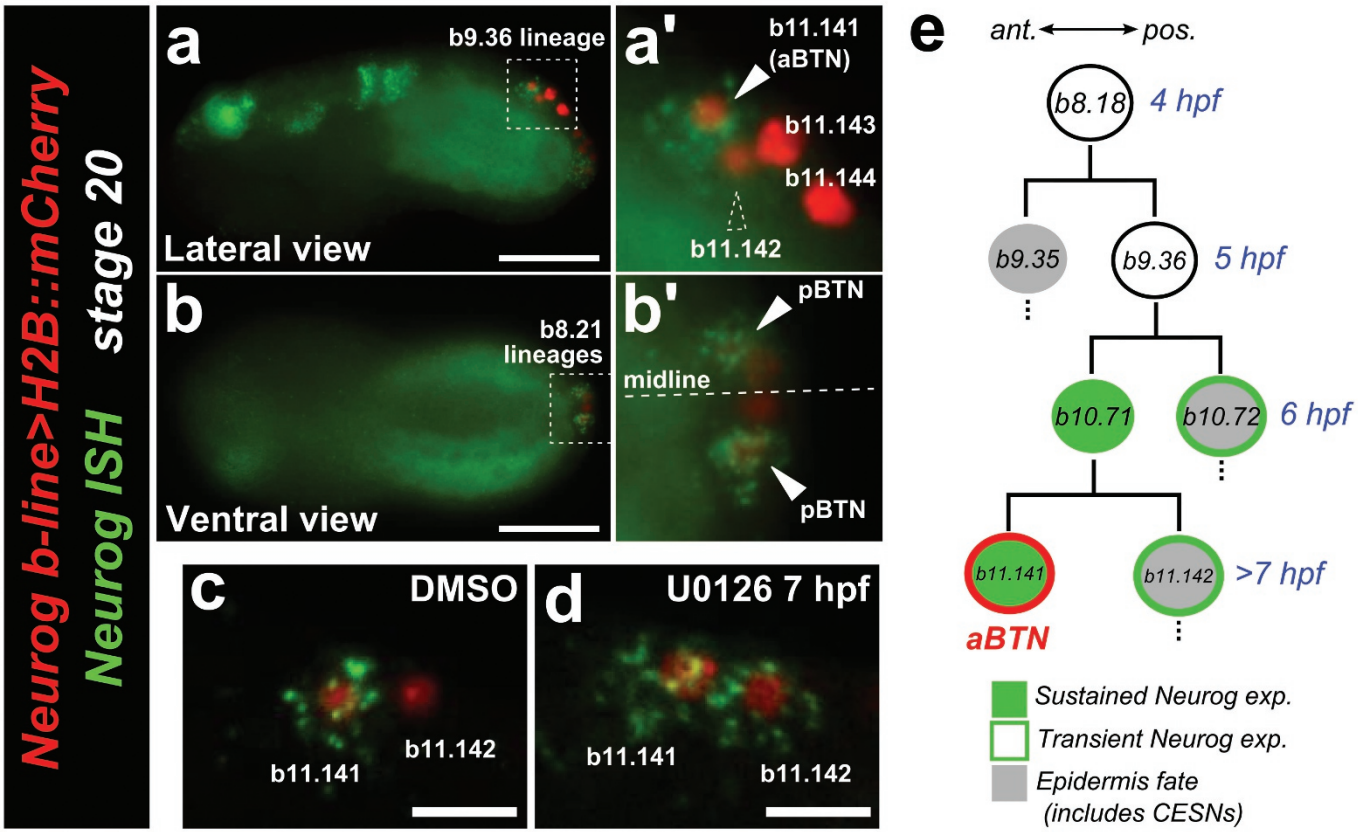

Extended Data Figure 4 | Spatiotemporal restriction of *Neurog* expression. **a**, Lateral view of *in situ* hybridization (ISH) for *Neurog* (green) in embryo electroporated with *Neurog b-line>H2B::mCherry* (red) shows that *Neurog* expression is selectively maintained in only a subset of initially *Neurog*-expressing neural plate border cells. **a′**, In the b9.36 lineage, the anterior-most cell (b11.141, solid arrowhead) is always the sole one to express *Neurog* at this stage, and will go on to become the anterior BTN. Dashed arrowhead indicates b11.142, the sister cell of b11.141, which has downregulated *Neurog* relative to its sibling. **b**, **b′**, The identities of the cells in the tail tip (presumed b8.21-derived) lineages are unclear, but *Neurog* is similarly restricted (arrowheads) to a single cell on either side of the midline, which we interpret as the definitive posterior BTNs. **c**, Control embryo treated with DMSO vehicle, showing wild-type pattern of *Neurog* expression only in b11.141. **d**, *Neurog* is expanded to b11.142 upon treatment with the MEK inhibitor U0126 at 7 h.p.f. This condition also results in specification of supernumerary BTNs, presumably due to expanded *Neurog* expression (see text for details). Thus, downregulation of *Neurog* in b11.142 also requires MEK/ERK signalling. **e**, Diagram of the aBTN lineage, descended from the b8.18 blastomere. Scale bars in **a**, **b**, 25 μm. Scale bars in **c**, **d**, 10 μm.

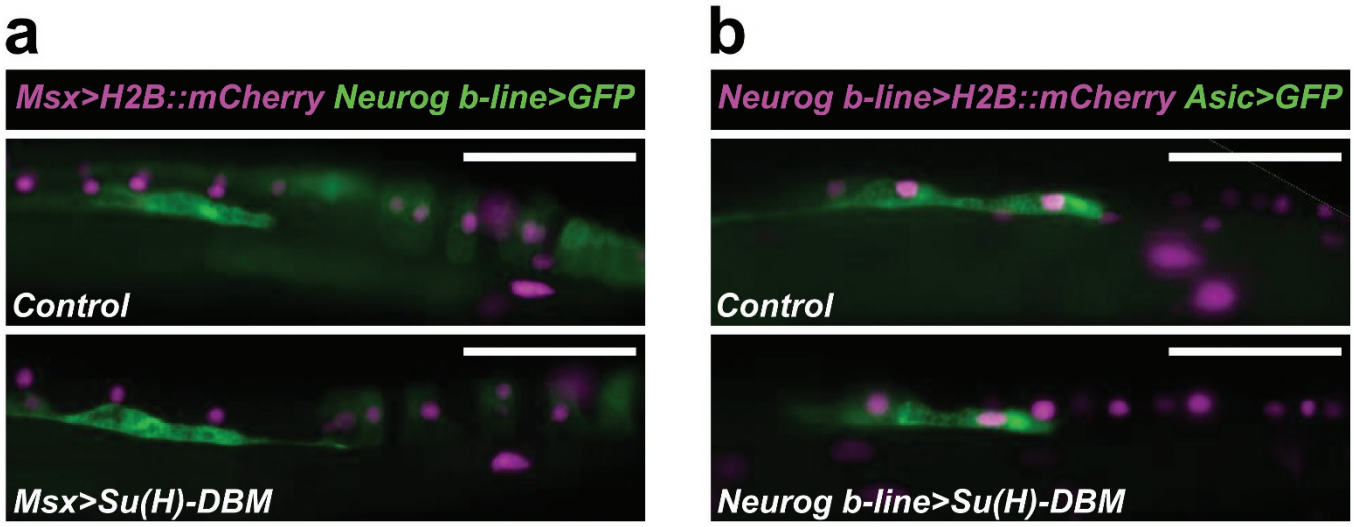

Extended Data Figure 5 | Perturbation of Notch signalling does not alter *Neurogenin* expression or bipolar tail neuron specification and differentiation. a, Top, lateral view of a stage 23 embryo electroporated with *Msx>H2B::mCherry* (magenta nuclei), *Neurog b-line>unc-76::eGFP* (green) and *Msx>nls::lacZ*, serving as the wild-type control condition. Bottom, embryo electroporated with same reporters as upper panel, plus *Msx>Su(H)-DBM,* which encodes a DNA-binding mutant form of the Notch co-activator Rbpj. No discernable difference in *Neurog* activation or BTN specification was observed between control and *Su(H)-DBM* conditions (1 of 32 versus 2 of 42 embryos showing ectopic *Neurog*$^{+}$ BTNs, respectively). **b**, Late overexpression of *Su(H)-DBM* using the *Neurog b-line* driver similarly did not alter BTN specification/differentiation, as monitored by *Asic>unc-76::eGFP* reporter expression (0 of 50 control versus 0 of 50 *Su(H)-DBM* embryos showed ectopic *Asic*$^{+}$ BTNs). Scale bars, 50 μm.

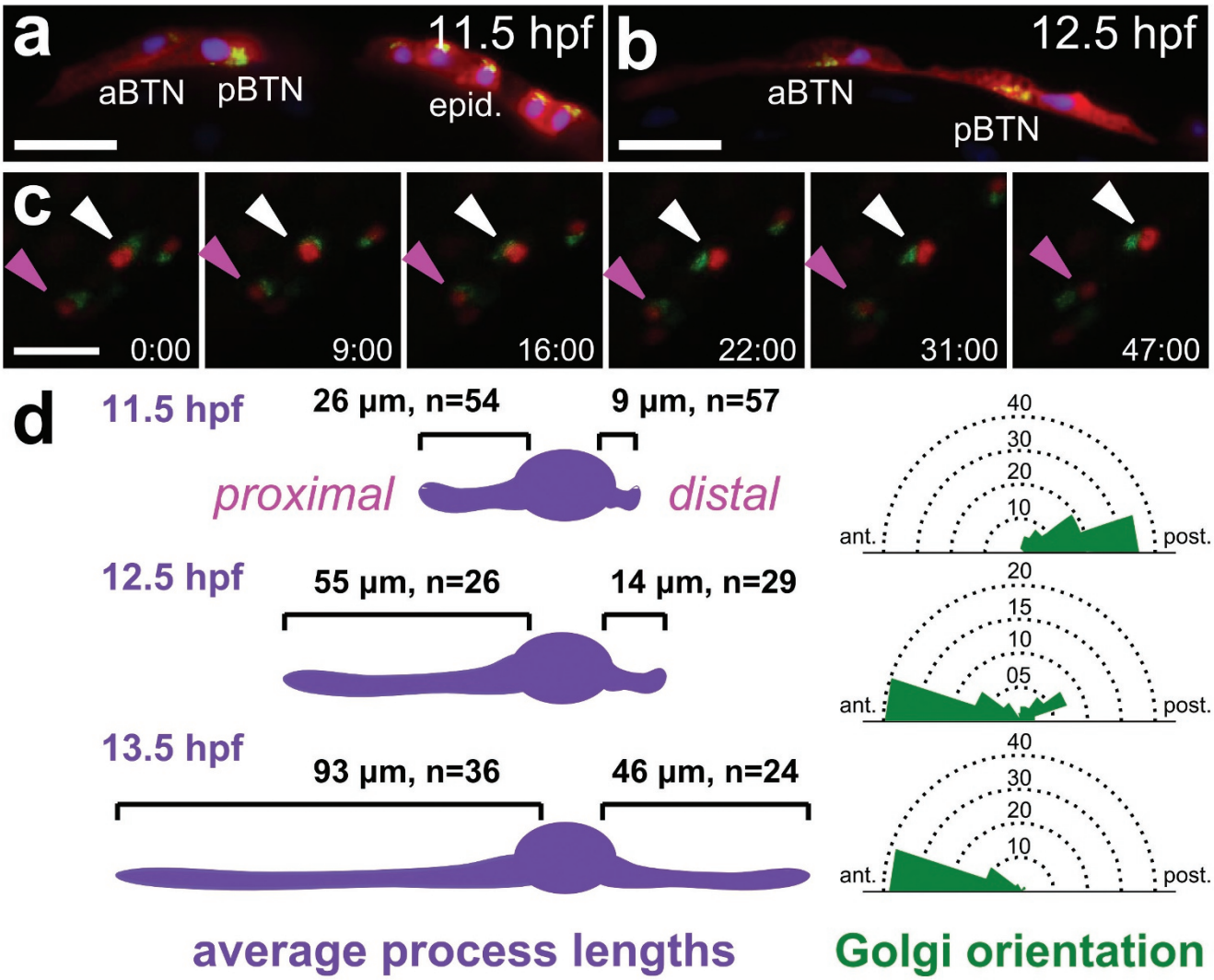

Extended Data Figure 6 | Cell polarity and morphogenesis of bipolar tail neurons. a, Embryo at 11.5 h.p.f. (18 °C) with BTNs displaced from clonally related epidermal cells (epid.) labelled by UNC-76::VenusYFP (red), Galnt7ΔC::CFP (green), and H2B::mCherry (blue) driven by *Neurog b-line cis*-regulatory module. Targeted localization of CFP by the Galnt7 N-terminal signal sequence reveals polarized subcellular distribution of Golgi apparatus on posterior side of BTN nuclei as migration and proximal process extend in an anterior direction. This is distinct from the apical (dorsal) location of the Golgi apparatus in epidermal cells. **b**, Embryo at 12.5 h.p.f. (18 °C) showing 180° inversion of Golgi apparatus localization to the anterior side of the nucleus, immediately preceding distal process extension. Scale bars in **a**, **b**, 50 µm. **c**, Still frames from a confocal image stack time lapse movie (Supplementary Video 4) showing inversion of Golgi complex (Galnt7ΔC::VenusYFP, green) relative to nuclei (H2B::mCherry, red) in migrating BTNs. Time lapse imaging initiated at 11.5 h.p.f. (18 °C). Time in minutes elapsed from start shown at bottom right of each panel. Anterior BTN (aBTN) indicated by magenta arrowhead, posterior BTN (pBTN) indicated by white arrowhead. Scale bar, 25 µm. **d**, Diagram showing correlation of average length of proximal (left) and distal (right) processes and angle of Golgi apparatus location relative to cell nucleus along the anterior–posterior axis in BTNs at different time points. Locations of Golgi apparatus represented by rose plots of bins of 20° spanning anterior (0°) and posterior (180°) endpoints around dorsal edge of BTN nucleus. Bin diameters indicate number of cells. Embryos analysed belong to the same pool as embryos in **a** and **b**. See Supplementary Table 1 for source data.

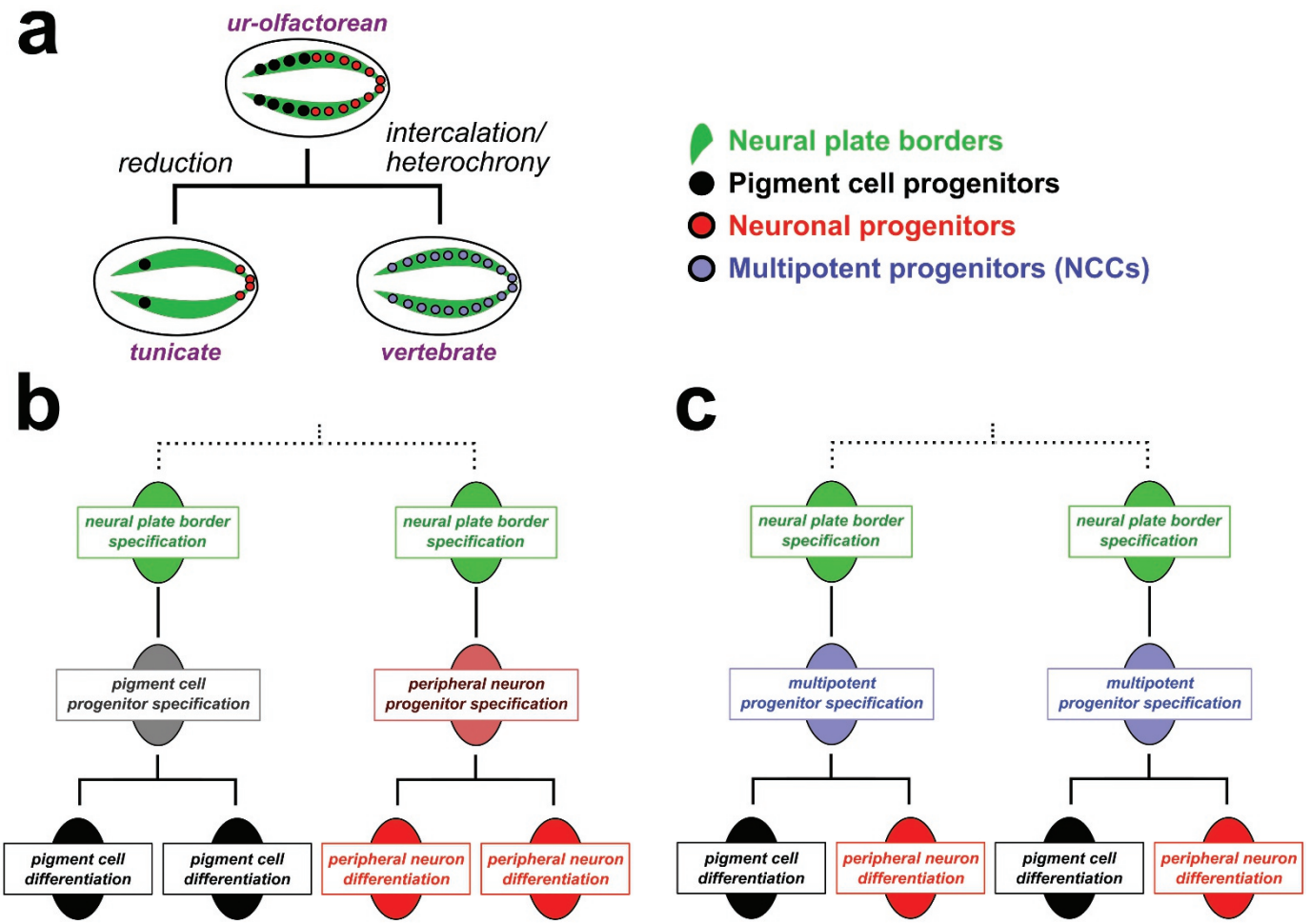

Extended Data Figure 7 | Proposed evolution of neural crest through the acquisition of multipotency by neural plate border cells. a, Cartoon diagram depicting a hypothetical path for neural plate border and neural crest evolution, starting with the reconstructed last common olfactorean ancestor, which could have had neural plate borders lined with committed progenitor cells giving rise to several pigmented ocelli and BTN-like peripheral neurons, a condition that may be conserved in extant cephalochordates[50]. These cells would have been reduced in the highly miniaturized embryos of extant tunicates, while vertebrates are proposed to have co-opted a mesenchymal, multipotency program to bestow these cells with the potential to give rise to pigment cells, peripheral neurons or other derivatives, after a prolonged period of EMT and migration. **b**, Diagram representing idealized cell lineages in the neural plate borders of tunicate and hypothetical urolfactorean ancestor, in which segregated lineages at the neural plate borders give rise to committed pigment cell or peripheral neuronal progenitors. **c**, Diagram of simplified neural crest cell lineage deploying a multipotency program downstream of neural plate border specification and upstream of cell differentiation. Thus, neural crest cells could have evolved through redeployment of a multipotency program (intercalation hypothesis)[1], or through its maintenance from earlier embryonic stages (heterochrony hypothesis)[30].

Extended Data Table 1 | Synaptic input from bipolar tail neurons to motor neurons, identified by electron microscopy

Postsynaptic motor neuron identity	Synapse partnership	Number of synapses	Total number of sections with synaptic profile
MN1 Left (A11.118)	BTN1-->MN1L	27	134
	BTN3-->MN1L	21	88
	Total	**48**	**222**
MN1 Right (A11.118)	BTN1-->MN1R	3	14
	BTN2-->MN1R	22	94
	BTN3-->MN1R	1	4
	BTN4-->MN1R	11	55
	Total	**37**	**167**
MN2 Left (A10.57)	BTN1-->MN2L	10	51
	BTN3-->MN2L	6	30
	Total	**16**	**81**
MN2 Right (A10.57)	BTN2-->MN2R	17	90
	BTN4-->MN2R	10	73
	Total	**27**	**163**
MN3 Left	BTN1-->MN3L	1	2
	Total	**1**	**2**
MN4 Left	BTN1-->MN4L	2	9
	Total	**2**	**9**
MN4 Right	BTN2-->MN4R	2	5
	BTN4-->MN4R	1	2
	Total	**3**	**7**
MN5 Left	BTN1-->MN5L	1	3
	Total	**1**	**3**
MN5 Right	BTN4-->MN5R	1	3
	Total	**1**	**3**

BTN, bipolar tail neuron. MN, motor neuron. Axons of BTN1 and BTN3 lie on the left hand side of the embryo, and BTN2 and BTN4 on the right. The axons are not traced to their somata to indicate which would be anterior and posterior.